

# MODELING THE NOISE EQUIVALENT RADIANCE REQUIREMENTS OF IMAGING SPECTROMETERS BASED ON SCIENTIFIC APPLICATIONS

Daniel Schlöpfer and Michael Schaepman

*Remote Sensing Laboratories, Department of Geography, University of Zurich*

*Winterthurerstr. 190, CH-8057 Zürich, Switzerland*

## ABSTRACT

The derivation of radiometric specifications for imaging spectrometers from the visible to the short-wave infrared part of the spectrum is a task to be based on requirements of potential scientific applications. A method for modeling the noise equivalent radiance at-sensor level is proposed. The model starts with surface reflectance signatures, transforms them to at-sensor signatures, and combines signatures of various applications with regard to performance requirements. The wavelength dependent delta radiances are then derived at predefined radiance levels using a model of the sensor performance. The model is applied with regard to the upcoming APEX imaging spectrometer system. A combination of various potential application disciplines forms the basis of the experiment. The results help in the definition of radiometric levels for laboratory calibration, of the noise equivalent radiance levels, the quantization of the signal, and the spectral range of an instrument to be designed.

OSIC Code: 280.0280 Remote sensing

## 1. Introduction

The performance of imaging spectrometer systems has been defined in the past mainly by technical constraints. As the technology has improved considerably, the question about the scientific requirements of such instruments has become more evident. In the definition phase of the Airborne Prism Experiment (APEX)<sup>1</sup>, the European Space Agency (ESA) thus initiated activities for derivation of scientifically based requirements for an airborne imaging spectrometer. APEX is an imaging spectrometer which is being built within the framework of the ESA PRODEX programme based on a Swiss-Belgian initiative. The system shall be capable of providing a vicarious calibration reference<sup>2</sup> for spaceborne instruments as well as demonstrating various imaging spectroscopy applications<sup>3</sup>.

The simulation of at-sensor signals can be done using forward simulation approaches<sup>4,5</sup>. These derived signatures are driven by assumptions on surface reflectance, geometric/atmospheric conditions, and sensor specifications. These three parts of any model need to be addressed on a physical basis for simulation of sensor performance.

An optimal modeling approach should only include minimal knowledge about the sensor system and its capabilities<sup>6</sup>. Some constraints have to be given initially such as the wavelength range and the spectral resolution. The forward radiometric sensitivity analysis is done using a predefined set of variables (representing scientific applications) to be selected according to their relevance. The underlying data basis is compiled using models based on inversion and assimilation techniques as commonly used in imaging spectroscopy. The critical at-surface delta reflectance is then upward-continued to at-sensor signals based on standard radiometric situations, avoiding extreme cases, whereas modeling uncertainties of the atmospheric propagation are not included in these analyses. Atmospheric signatures may overlay surface signatures within gaseous absorption bands or influence the absolute radiance level for low wavelengths due to path radiance effects. The influence of such uncertainties will decrease for upcoming instruments, as atmospheric correction of imagery will be possible to a high level of accuracy<sup>7</sup>.

This approach includes a reflectance data basis that has been derived using models suitable for inversion and/or assimilation approaches<sup>8,9</sup>. However, the unambiguous definition of the radiometric performance of a new imaging spectrometer is limited using these techniques since most inversion techniques have been developed based on existing instruments. The presented approach concentrates on the analysis of at-sensor radiance signals, leaving the method of parameter retrieval (including the derivation of spectral resolution requirements) open to other scientific approaches to this problem. The intention is to derive the radiometric performance requirements for a number of given spectroscopic signatures which knowingly can be resolved at the spectral resolution typical to imaging spectrometers.

## **2. Methodology**

A schematic view of the modeling concept is outlined in Figure 1. Three main parts can be distinguished within this model:

- reflectance model: calculation or measurement of application-specific surface reflectance signatures for each selected variable,

- radiance model: forward modeling of at-sensor radiance and delta radiance signatures, and
- sensor model: transformation of at-sensor signatures into noise equivalent radiance values.

*[place Figure Here]*

The herewith resulting delta radiance values ( $\Delta L$ ) are directly transformed to *NedL* (Noise equivalent delta radiance) values and SNR (Signal to Noise Ratio) values for the definition of a sensor. Note that the term *NedL* is used as descriptor for the sensor performance. The delta radiance  $\Delta L$ , on the other hand, describes critical variable-specific radiance signatures which do not depend on the noise level of a sensor.

The environmental conditions, operational constraints, and geometrical presuppositions for imaging spectrometry data acquisition must be defined before this method can be applied. Taken together, they define a ‘model scenario’. Most prominent parameters in a model scenario are: season, daytime, surface elevation, flight altitude, spatial resolution, spectral range, maximum spectral resolution, location, view angles, air temperature, and cloud coverage. An average scenario is proposed as baseline for all parameters. This standard scenario is helpful for intercomparison of the signals for various applications under the same environmental conditions and with the same solar illumination conditions. In any case, this standard scenario will not fulfill all conditions at one time. Additional application specific scenarios will have to be defined for a realistic simulation of the expected signal range.

## 2.1 Reflectance Model

The reflectance data is derived from application-specific established scientific models or from field and laboratory measurements, typically at 1 nm resolution. The full range of parameter variation is taken into account while each parameter is varied by the required retrieval accuracy to obtain a second entity of reflectance spectra augmented by the critical delta reflectance ( $\Delta\rho$ ). The concentration change to be detected per variable is derived from the needs of data end users. All surface reflectance spectra are simulated at typical irradiance levels and directions to account for illumination and BRDF effects.

A typical set of reflectance data is thus given as follows

$$\rho_{\lambda,a} = \rho(p_i, \lambda, \theta) , \text{ and } \rho'_{\lambda,a} = \rho'(p_i + \Delta p_i, \lambda, \theta) = \rho_{\lambda,a} + \Delta\rho_{\lambda,a} , \text{ where } i = 1, \dots, n , \text{ and (1)}$$

$$p_i = \{p_{i,1}, p_{i,2}, \dots, p_{i,m_i}\}, \text{ and } \Delta p_i = \{\Delta p_{i,1}, \Delta p_{i,2}, \dots, \Delta p_{i,m_i}\}. \quad (2)$$

$n$  is the number of parameters per application  $a$ ,  $p_i$  are the individual parameters  $i$  of application  $a$ ,  $\Delta p_i$  are the critical detection limits for parameters  $i$ ,  $m_i$  is the number of discrete values of parameter  $p_i$ ,  $\lambda$  is the wavelength center of each basic spectral band (i.e. resolved at 1 nm intervals), and  $\theta$  is the solar zenith angle (incidence angle). The set finally consists of  $(n+2)$ -dimensional reflectance data, including all cross sensitivity effects between the  $n$  parameters and the sun zenith angle, per wavelength.

## 2.2 Radiance Model

The reflectance signatures as of expression (1) are then transferred to at-sensor radiances using the MODTRAN4 radiative transfer code<sup>10</sup> following an initially defined model scenario. The MODTRAN4 radiative transfer code outputs are formatted and analyzed using the MODO utility<sup>11</sup>. Some assumptions on generic sensor characteristics have to be used in this step which include the potential spectral range, resolution, and sampling interval. A low sampling interval (e.g. 1nm) is recommended to take into account the undefined position of each spectral band at this point of the definition phase. The spectral resolution ('full width at half maximum'; FWHM) on the other hand is first taken at the lowest potential value of the instrument under investigation. It may later be iteratively reduced for optimization of the sensor design.

Given a number of fixed parameters in tuple  $\{S_c\}$  of a model scenario, the simulated radiance may be written as:

$$L_{\lambda,a} = L(\{\rho_{\lambda,a} | \rho'_{\lambda,a}\}_{S_c}) = L(p_i, \Delta p_i, \lambda, \theta)_{\{S_c\}}, \quad (3)$$

where  $\lambda$  represents the central wavelength of the synthetic spectral band at fixed FWHM resolution. The critical delta radiance ( $\Delta L$ ) can now be inferred as difference between radiance levels of a parameter variation:

$$\Delta L_{\lambda,a} = |L(\rho'_{\lambda,a})_{\{S_c\}} - L(\rho_{\lambda,a})_{\{S_c\}}|. \quad (4)$$

The relation between the delta radiance signature and the radiance is now given as pairs:

$$\{L | \Delta L\}_{\lambda,a} = \{L(p_i, \lambda, \theta)_{\{S_c\}} | \Delta L_{\lambda,a}\}. \quad (5)$$

The radiance values summarized by expression (3) are used to derive generic minimal, median, and maximal radiance levels based on all variables per application.

### 2.3 Sensor Model

The derivation of normalized signatures requires that all application/variable requirements given by pairs  $\{L|\Delta L\}_{\lambda, a}$  be normalized to specified radiance levels. A sensor model is used to transfer these pairs to  $L/NedL$  requirements. The approach is defined as follows:

- fit a generic photon-noise limited function to all modeled  $L/\Delta L$  pairs per wavelength and variable,
- select the most demanding case of all relevant situations,
- derive spectral NedL values at the three specified radiance levels (minimum, median, maximum) per variable,
- exclude non-significant wavelength ranges, and
- combine the signatures to overall radiometric requirements.

This result is then evaluated for SNR and  $NedL$  based on the median radiance level. The concept is based on the assumption that the radiometric resolution of an instrument (given by  $NedL$ ) should be equal to or better than the signatures  $\Delta L$ .

#### Normalization of Delta Radiance Values

The individual values of  $\Delta L$  all depend on a specific absolute radiance value. For every variable, the most demanding combination needs to be searched for from all simulated  $L/\Delta L$ -pairs. A square-root function is fitted to every single point for this purpose. It is derived from the fact, that the noise  $\sigma$  of a sensor increases with the square root of the number of electrons at a photocathode:<sup>12</sup>

$$\sigma(S_{c,t}) = \left[ \Phi_p Q \tau + \frac{I_{dc}}{e} \tau \right]^{1/2} \text{ [electrons]}, \quad (6)$$

where  $S_{c,t}$  is the total at-sensor signal,  $I_{dc}$  is the dark current,  $\Phi_p$  is the incoming photon flux,  $Q$  is the quantum efficiency, and  $\tau$  is the integration time. The dark current term in equation (6) may be omitted under the assumption that the number of noise electrons produced by the incoming radiation (i.e. the ‘shot noise’) is significantly larger than the number of dark current electrons. Furthermore, it is assumed that the measured radiance  $L_\lambda$  is linearly related to the number of photons:

$$L_\lambda = n_\lambda \Phi_p Q \tau, \quad (7)$$

where  $n_\lambda$  is a factor which linearly relates the radiance level to the number of measured electrons. The shot noise in terms of at-sensor radiance can thus be given as:

$$\sigma(L_\lambda) = \sigma(n_\lambda \Phi_p Q \tau) = n_\lambda [\Phi_p Q \tau]^{1/2} = n_\lambda \left[ \frac{1}{n_\lambda} L_\lambda \right]^{1/2} = [n_\lambda L_\lambda]^{1/2}. \quad (8)$$

The detectability is given by the smallest signatures to detect, i.e.  $\sigma(L_\lambda) \leq \Delta L_\lambda$ . Therefore one can write for the limiting case:

$$\Delta L_\lambda = [n_\lambda L_\lambda]^{1/2}, \text{ and } n_\lambda = \frac{(\Delta L_\lambda)^2}{L_\lambda}. \quad (9)$$

The signature pairs where  $n_\lambda$  is minimal are the most critical ones and thus are selected per variable. The corresponding square root function represents a lower hull to the cloud of all situations simulated per variable and is calculated for each discrete wavelength of the data tuples as given in Eq. (5). An example for one variable at one specific wavelength is given in Figure 2.

*[place Figure 2 here]*

As mentioned above, the dark current noise is not included in this assumption and may add up as a constant value to the shot noise function. Omitting dark current however is justified since it is only of relevance for low radiance conditions whereas at high radiance the photon noise is the dominant factor<sup>12</sup>. This argument also leads to the conclusion that any further evaluation based on the given ‘square-root’-rule should be based on medium to high radiance levels and not on minimum radiance.

### **Exclusion Process**

The method described so far allows the calculation of  $\Delta L$  to  $L$  relations for all variables at any radiance level. If the signatures of all variables need to be combined for an overall view of the radiometric requirements, a clearly defined exclusion process is required to narrow the critical wavelength ranges per variable and to derive a combined result. For automation of the calculation, an analytical selection procedure is searched for rather than selecting critical wavelength ranges purely based on scientific knowledge of experts.

The wavelength selection approach proposed in this paper uses the relative signature strength  $S_{rel}$  per wavelength. This value can be defined based on the radiance signatures ( $Sig$ ):

$$Sig(\lambda) = \frac{\Delta L_\lambda}{L_\lambda}, \text{ and } S_{rel} = \frac{Sig(\lambda)}{\max(Sig(\lambda))}. \quad (10)$$

A limit  $l$  is then defined which excludes all signatures at wavelengths where  $S_{rel}$  is lower than this limit. The selection of relevant  $\Delta L_\lambda$ -signatures is thus given by

$$\Delta L_{\lambda, S} = \begin{cases} \Delta L_\lambda & \forall (S_{rel} \geq l) \\ \text{undefined} & \forall (S_{rel} < l) \end{cases}. \quad (11)$$

The exclusion limit  $l$  is an important factor for the combination of heterogeneous signatures. The analysis of various spectral data sets<sup>14</sup> showed that  $l = 0.2$  is a suitable limit preserving spectral features while excluding non-significant signatures. Thus, this value has been fixed for further analysis.

### Combination process

The signatures of all applications and variables have to be combined for the derivation of final noise equivalent radiance requirements. The combination is done based on the delta radiance values remaining after the exclusion process:

$$\Delta L_{\lambda, S}^m = \min(\Delta L_{\lambda, S, i})|_{i=0, k_\lambda}, \quad (12)$$

where  $\Delta L_{\lambda, S, i}$  is the delta radiance per wavelength and per valid (non-excluded) variable  $i$ . The variable  $k_\lambda$  is the number of variable signatures available per wavelength. No value can be derived on wavelengths where none of the variables shows a significant delta radiance value.

At this point, the resulting signatures can be transferred to noise equivalent radiance requirements with

$$NedL \leq \Delta L_{\lambda, S}^m, \quad (13)$$

which connects sensor performance and radiometric requirements. In relation to the absolute radiance levels, the signal to noise ratio ( $SNR_\lambda$ ) can now be defined such that

$$\text{SNR}_\lambda = L_\lambda / \text{Ned}L \geq L_\lambda / \Delta L_{\lambda, S}^m . \quad (14)$$

The concept is based on a hypothetical sensor with fixed spectral resolution. A variation of the spectral resolution could be introduced in the radiance model (section 2.2) where the at-sensor radiance is convolved to the standard resolution. Such a change would propagate through the whole process and would influence the results significantly.

### 3. Example

The model as described above is applied to a scientific data set for the definition of APEX sensor performance<sup>14</sup>. Six different topics of interest have been chosen for the inclusion in the sensitivity analysis as listed in Table 1. The calibration application is included since one of the main goals of APEX is being capable of cross-calibration and validation of spaceborne instruments. It is treated in parallel to the other applications, since calibration affects the whole wavelength range and by definition imposes the highest requirements in comparison to each individual application.

*[place Table 1 here]*

A few technical restrictions apply which are intrinsic to airborne pushbroom imaging spectrometers or are an initial postulation for the APEX system. These constraints are mainly the sensor FOV being not more than 28 degrees, the wavelength range between 380 and 2500 ( $\pm 30$ ) nm, and the spectral resolution at best not better than 2 nm. The degree of freedom for the definition of the standard scenario is high concerning atmospheric conditions, flight heading, and solar zenith angle. Given the low FOV of the investigated design, a sensor zenith of 0 degree is assumed. Larger sensor zenith angles, e.g., for BRDF analyses, could only be achieved by introducing a tilted sensor<sup>22</sup> which is not further considered here.

The sensor altitude is defined by the restrictions on FOV and spatial coverage/resolution (i.e. 1000 pixels across track at 0.5 mrad spatial sampling interval). The aircraft furthermore needs to be above the turbulent boundary layer if the data are used for validation of spaceborne instruments. Given these facts and the need for a high spatial coverage, a flight altitude of 4-10 km is desirable, while a standard altitude at 7.5 km a.s.l. has been chosen. The second major parameter relevant for the radiance levels is the



sun zenith angle which mainly affects the solar illumination. A standard situation 1st of June at noon has been selected for definition of the solar angles. The latitude of data acquisition may vary between Equator and northern conditions between 0 and 70°, resulting in sun zenith angles between 0 and 55° where from 18° and 48° are selected as standard cases. The high latitudes have to be taken into account due to potential snow and water applications in northern countries. Additionally, the following items have been defined in the model scenario: atmospheric model (Midlatitude Summer), boundary temperature (293.15 K), ground elevation (0.2 km), aerosols (rural, visibility 23 km), scattering simulator (Isaac 2-Stream<sup>13</sup>), no clouds. As mentioned above, certain application-specific scenarios can be taken into account in addition to this standard scenario for more realistic radiometric simulation.

In general, input signatures to the the model are reflectance spectra, except for atmospheric applications and calibration, where the at-sensor radiance (or delta radiance) is provided directly. In the following, the modeling procedure for vegetation is briefly described. The setup of all other models was done analogous to the vegetation model<sup>14</sup>.

### **3.1 Reflectance Signatures**

The vegetation reflectance spectra are modeled for three variables: leaf chlorophyll, leaf water, and leaf area index. For the simulation, the PROSPECT/SAIL<sup>15,16</sup> approach has been chosen which combines a leaf reflectance model with a bi-directional canopy model. A 4-dimensional LUT is built including variation in sun zenith angle at 0, 18, and 48° (which influences the BRDF behavior of the spectra) between 400 and 2400 nm at 1 nm resolution. The LUT contains the directional surface reflectance under realistic irradiance conditions according to the model scenario. The modeled reflectance spectra and the respective delta reflectance for leaf chlorophyll are shown in Figure 3.

*[place Figure 3 here]*

A relative accuracy of all parameters of 10% (at every level) is considered as critical variation and is then modeled on all levels of parameters, being 25, 45, and 70  $\mu\text{g}/\text{cm}^2$  for leaf chlorophyll; 5, 10, and 20  $\text{mg}/\text{cm}^2$  for leaf water (Cw), and 0.5, 2 and 6 for leaf area index. The canopy boundary conditions for the simulation were structure parameter:  $N=1.5$ , dry matter:  $1.25 * Cw$ , leaf angle inclination: 58°, hot spot parameter: 0.1.

### 3.2 Radiance Signatures

All reflectance spectra are transferred to at-sensor spectral radiance as described in Section 2.2. The results are convolved to a standard resolution of 7.5 nm at FWHM, corresponding to the 5 nm sampling interval which is the lower technical limit expected in the APEX system.

A direct comparison of the derived signatures between application must be made with care, since the  $\Delta L$  -values are not derived at the same radiance levels (compare Figure 3). The subsequent normalization is thus indispensable for intercomparison of the signatures on common radiance levels. In Figure 4, all  $L/\Delta L$  -pairs are plotted for the three vegetation variables at two selected wavelengths. The lowest shot noise limited square-root function is shown for each variable, one being almost coincident to the x-axis. Insignificant signatures (with almost disappearing functions) are later excluded from further analysis at the respective wavelengths.

*[place Figure 4 here]*

The derived functions through the most critical respective data points are used to normalize the signature to the median radiance level. The top graph of Figure 5 shows the results of this procedure if the delta radiance values are extracted for the three vegetation variables. The median radiance level is a spectrum representing a typical vegetation spectrum in the depicted case but could also be a constant which is better suited for calibration purposes. In any case, the qualitative information contained in this  $\Delta L$  values does not depend on the chosen radiance level. The noisy appearance of the curves is due to modeling noise and an amplifying effect of the described normalization procedure.

### 3.3 Sensor Model

The such derived and normalized signatures need now to be combined to derive generic requirements. Variables of low significance are excluded per wavelength in order to achieve realistic requirements. An example of the automatic exclusion process for vegetation analysis based on the selected 20% level is given in Figure 5. Only wavelengths with signatures above one fifth of its maximum are included. Thus, a lower level (e.g. 10%) would lead to stricter requirements on the delta radiance signatures than the 20% level does. An optimal exclusion level preserving the major (known) diagnostic spectral features is searched for by analyzing the results on levels between 5 and 50%. The major features for all variables

are clearly extracted from the whole signature spectra using the 20% level. For levels higher than 20%, major features would be excluded for certain variables (e.g., for leaf water in vegetation).

*[place Figure 5 here]*

## **4. Results**

The analysis has been made for all variables as of Table 1 and the resulting values are analyzed for dynamic range, wavelength range, and noise equivalent radiance for an airborne imaging spectrometer such as APEX.

### **4.1 Dynamic Range**

Minimum, median, and maximum radiances are first derived for each application. Furthermore, the minimum and maximum expected radiance at a 0 and 100% reflecting target is included. The generic minimal, median, and maximal radiance levels are combined from the corresponding applications specific values as wavelength dependent absolute minimum, generic median, and absolute maximum for all applications. The median value is taken as median of all application-specific medians, since all applications can be weighted equally only by this kind of combination. The signature for limnology is only considered up to 800 nm due to the almost zero reflectance of water at higher wavelengths (where the model was run up to 1099 nm). For the same reasons, the snow application is only considered up to 1500 nm. The resulting generic radiance levels are plotted in Figure 6. The calibration requirements only have been used for the derivation of the lowest radiance level where the absolute minimum of the other applications was well above the calibration level after exclusion of snow and limnology for the above-mentioned wavelength ranges. The 0% and 100% reflecting target as well as the maximum calibration requirement are added for cross-comparison in the plot, describing the theoretical dynamic range.

*[place Figure 6 here]*

The dynamic range of an instrument such as APEX should cover all potential applications as well as the dynamic range that is required for the cross-calibration of other instruments. The minimum radiance capabilities usually should start at zero, although it might be useful to restrict the minimum radiance to higher radiance levels in the visible part of the spectrum where atmospheric path radiance is a predominant constant additive term to the total radiance. The application-derived minimum radiance level is above an absolute minimum for longer wavelengths due to the seldom encountered dark targets in this wavelength range.

The maximum at-sensor radiance that is expected is coupled to the saturation level of an instrument and should not be saturated for the application scenarios. The application-derived radiance value in the VIS/NIR part of the spectrum is in good agreement with the absolute maximum as derived from MODTRAN4 (at 100% reflectance) and the values defined for calibration purposes (see Figure 6). In the SWIR part of the spectrum, the absolute maximum of all applications is about 30% lower than the signal of a 100% reflecting target under optimal (i.e. maximal) conditions. It is recommended using the maximum MODTRAN spectrum in the SWIR spectrometer rather than the maximum applications spectrum for the derivation of a sensor saturation level. Otherwise, some currently not included mineralogical (or similar) applications might not be covered by the sensor capabilities. For the visible part of the spectrum, the required maximum radiance is in the range of  $0.3$  to  $0.6 \text{ W m}^{-2} \text{ sr}^{-1} \text{ nm}^{-1}$ , whereas in the NIR radiances between  $0.07$  and  $0.2$  apply. In the SWIR part of the spectrum, the required maximum is between  $0.01$  and  $0.03 \text{ W m}^{-2} \text{ sr}^{-1} \text{ nm}^{-1}$ .

## **4.2 Delta Radiance Requirement**

The overall delta radiance requirement is derived as described in Section 2.3. Figure 7 shows the combination of all delta radiance values at median radiance levels as of Figure 6. The signatures have been smoothed using a 30 nm wide filter in order to remove modeling noise. The evaluation of these requirements is preferably done on the median radiance level since the extrapolations involved in using any other radiance level (minimum or maximum) increases the uncertainty of the final results substantially against the median case. Averaging of independent requirements for various applications on the other hand is not appropriate since variables with very strong signatures override any other potential applications (e.g., the low requirements for snow applications would obstruct potential vegetation applications

in the NIR). However, if the focus of a sensor is on one specific applications the whole analysis can be adapted to this application specific levels.

*[place Figure 7 here]*

### **4.3 SNR Requirements**

The number most often used for sensor performance definition is the signal to noise ratio (SNR). SNR values are provided based on the given scientific validation at the median radiance level. The clear definition of this level is indispensable in order to avoid the often encountered confusion about SNR values. The final results have been smoothed by a 30 nm wide filter. As already mentioned in Section 3.3, the signature exclusion level influences the final sensor requirements. Figure 8 shows the influence of exclusion levels  $l$  between 10 and 30% on the final SNR demand at median radiance. The 20% level proves to be of low sensitivity to further increases of  $l$ , while lower exclusion levels would increase the sensor requirements substantially. The selection of the 20% level can thus be confirmed as a realistic presupposition.

The SNR requirement and the original driver applications are plotted in Figure 9. On median radiance level, the SNR varies in the range between 100 and 2000 for the VIS/NIR detector. The high SNR requirements in the visible part of the spectrum are driven mainly by limnology and snow applications. This wavelength range therefore needs special attention in sensor design. The performance in the SWIR wavelength part on the other hand can be constant at an SNR between 100 and 300. It is recommended to cross-compare any sensor requirements derived from these SNR curves with the values given in Figure 8, which show a more generic view of the problem by including a range of exclusion criteria.

*[place Figure 8 here]*

### **4.4 Wavelength Range**

Figure 9 gives an impression about the wavelength range to be covered by an imaging spectrometer. It is clearly shown that a continuous spectral coverage is highly desirable except for the 1850 nm SWIR water vapor absorption band (i.e. 1800-1920 nm), where no significant signatures have been found. The

lower limit of relevant signatures is at least at 400 nm. As most models used for this analysis did not take into account lower wavelengths, the real lowest limit of interest may be substantially lower than this model limit. Recommendations from consulting experts (c.f., acknowledgements)<sup>14</sup> have shown that a coverage starting at 300-350 nm would have benefits, specifically for atmospheric applications. For the upper spectral limit, critical geological signatures have been detected up to 2450 nm which definitively need to be detected by a sensor.

*[place Figure 9 here]*

## 5. Conclusions

A complete model for the analysis of the variable specific relation between radiance and delta radiance has been proposed and implemented. The approach consistently determines  $NedL$  at predefined radiance levels. In this paper, the analysis was done on a generic median radiance level, but the delta radiance requirements may also be calculated at any radiance levels to fit, e.g., the characteristics of laboratory radiance sources during calibration. Moreover, the data basis allows recommendations on dynamic range, spectral range, or on radiometric quantization. It can be easily extended with additional applications or variables while the type of sensor can be adapted as well (e.g., satellite, ground-based) since the model presented is generic and constraints are sparse with respect to inherent system capabilities.

An underlying problem is that the radiative transfer code is run in a forward mode and that the inversion using real data relies on assumptions and measurements of the atmospheric state. Hence, a safety margin on top of the given values must be included when translating the requirements into system engineering specifications to take atmospheric uncertainties into account. Since the knowledge of the consultants in choosing relevant variables played a major role in the definition phase, it is not surprising that the achieved results are close to the state-of-the-art in imaging spectroscopy. Special attention must therefore be focused on the fact that existing models might limit themselves in the input quality for this modeling approach.

At this stage of the model implementation, we are assuming that all applications are treated at the same spatial scale. But the consideration of different spatial scales could be of significant interest in space related imaging spectrometers, since they often are a compromise between revisit frequency, download capability, and the number of spectral bands. Furthermore, no suitable indicators defining the spectral resolution of an instrument can be calculated using this model. Specific analysis of narrow band spectral signatures including the inversion process would be required to come to a thorough recommendation on this problem.

The presented model has the potential to be expanded with additional variables and applications. It can also be run for different sensors operating at different altitudes or with different spectral response characteristics. The method shall therefore be applied to other upcoming imaging spectrometers (e.g. ESA's 'Spectra' Instrument<sup>23</sup>) with specific application requirements. The inversion of the presented model is limited by the problem of acquiring simultaneous information of atmospheric in-situ data. It is therefore envisaged to integrate the overall uncertainty of atmospheric compensation into the model. This would then close the loop and a complete model including the inversion from at-sensor data to surface characteristics could be made available for the transformation of scientific requirements into engineering specifications.

## **6. Acknowledgements**

Valuable input to the scientific data basis of this study has been given by Frédéric Baret (INRA, F), Joachim Hill (University of Trier), Hermann Kaufmann and Karl Segl (GFZ Potsdam, GER), Peter Keller (MeteoSchweiz, CH), Jens Nieke (NASDA, JP), and Thomas Painter, (Univ. Calif. Santa Barbara, USA). The anonymous reviewers are thanked for their useful inputs to this paper. This work has been carried out under ESA/ESTEC Contract–No. 14906/00/NL/DC. Special thanks go to Michael Berger, Steven Delwart, Roland Meynard, and Gerd Ulbrich from ESA/ESTEC.

## REFERENCES

- <sup>1</sup> K.I. Itten, M. Schaepman, L. De Vos, L. Hermans., H. Schlaepfer, and F. Droz, "APEX-Airborne Prism Experiment a New Concept for an Airborne Imaging Spectrometer," in *Proceedings of the Third International Airborne Remote Sensing Conference and Exhibition*, B.J. Petoskey ed., (ERIM International Inc., Copenhagen DK, 1997), Vol. I, pp. 181-188.
- <sup>2</sup> M. Schaepman, and S. Dangel, 2000: "Solid laboratory calibration of a non-imaging spectroradiometer," *Appl. Opt., OSA*, **39**, 3754-3764.
- <sup>3</sup> D. Schläpfer, M. Schaepman, S. Bojinski, and A. Börner, 2000: "Calibration Concept for the Airborne PRISM Experiment (APEX)," *Can. J. of Remote Sens*, **26(5)**, 455-465, (2000).
- <sup>4</sup> R. Richter, "Model SENSAT: A Tool for Evaluating the System Performance of Optical Sensors," in *Propagation Engineering III*, L.R. Bissonnette and W.B. Miller eds., Orlando, Proc. SPIE **1312**, 286-297 (1990).
- <sup>5</sup> A. Börner, L. Wiest, P. Keller, R. Reulke, R. Richter, M. Schaepman, and D. Schläpfer: "SENSOR: A tool for the simulation of hyperspectral remote sensing systems," *ISPRS J. Photogramm. Remote Sens.*, Elsevier, **55**:299-312 (2001).
- <sup>6</sup> S. Blonski, C. Cao, J. Gasser, R. Ryan, V. Zanoni, and T. Stanley: "Satellite Hyperspectral Imaging Simulation," In *Proceedings International Symposium on Spectral Sensing Research ISSSR 1999, Las Vegas, USA, 1-4 November 1999*, A.J. Bruzewicz ed., (United States Corps of Engineers, Hanover, New Hampshire, USA, 2000), CD-ROM.
- <sup>7</sup> R. Richter, and D. Schläpfer, 2002: "Geo-atmospheric processing of airborne imaging spectrometry data. Part 2: Atmospheric/Topographic Correction," *Int. J. Remote Sens.* (to be published).
- <sup>8</sup> G. P. Asner, C. A. Wessman, D. S. Schimel and S. Archer, "Variability in Leaf and Litter Optical Properties: Implications for BRDF Model Inversions Using AVHRR, MODIS, and MISR," *Remote Sens. Environ.* **63**, 243-257 (1998).
- <sup>9</sup> M.H. Weiss, H. Chauki, D. Troufleau, and F. Baret, "Coupling canopy functioning and canopy radiative transfer models for remote sensing data assimilation," *Agric. For. Meteorol.*, **108(2)**:113-128 (2001).
- <sup>10</sup> A. Berk, L.S. Bernstein, and D.C. Robertson, *MODTRAN: A Moderate Resolution Model for LOWTRAN7* (Air Force Geophysics Laboratory, Hanscom AFB, MA, GL-TR-89-0122, 1989).
- <sup>11</sup> D. Schläpfer, "MODO: An interface to MODTRAN for the simulation of imaging spectrometry at-sensor signals," in *Proceeding 10th JPL Airborne Earth Science Workshop, February 2001*, Rob Green ed., (JPL, Pasadena, Calif., 2001), JPL 02-1, pp. 343-350.
- <sup>12</sup> H.J. Kostowski, 1997: *Reliable Spectroradiometry*, (Spectroradiometry Consulting, Maryland, USA,



ISBN 0-9657713-0-X, 1997), pp. 276 ff.

- <sup>13</sup> R.G. Isaacs, W-C. Wang, R.D. Worsham, and S. Goldenberg, “Multiple scattering LOWTRAN and FASCODE models”, *Appl. Opt.* **26**:1272-1281 (1987).
- <sup>14</sup> M. Schaepman, D. Schläpfer, K. Itten, P. Strobl, W. Mooshuber, A. Müller, W. Debruyn, I. Reusen, and D. Fransaer, *Performance and Calibration Requirements for APEX*, (Final Report ESA/ ESTEC Contract–No. 14906/00/NL/DC, RSL, University of Zurich, 2001), CD-ROM.
- <sup>15</sup> S. Jacquemoud and F. Baret, PROSPECT: A Model of Leaf Optical Properties Spectra. *Remote Sens. Environ.* **34**, 75-91 (1990)
- <sup>16</sup> W. Verhoef, “Light Scattering by Leaf Layers with Application to Canopy Reflectance Modeling: The SAIL Model.”. *Remote Sens. Environ.*, Elsevier, **16**, 125-141 (1984).
- <sup>17</sup> G. P. Asner, 1998: “Biophysical and Biochemical Sources of Variability in Canopy Reflectance,” *Remote Sens. Environ.*, Elsevier, **64(3)**, 234-253 (1998).
- <sup>18</sup> P. Keller, 2001: *Imaging Spectroscopy of Lake Water Quality Parameters* (Remote Sensing Series, RSL, Zürich, Switzerland, Vol. 32, 2001).
- <sup>19</sup> T.H. Painter, D.A. Roberts, R.O. Green, and J. Dozier, “Improving mixture analysis estimates of snow-covered-area from AVIRIS data,” *Remote Sens. Environ.*, Elsevier, **65(3)**, 320-332 (1998).
- <sup>20</sup> J.W. Boardman, “Inversion of high spectral resolution data,” in *Imaging Spectrometry of the Terrestrial Environment*, Proc. SPIE **1298**, 222-233 (1990).
- <sup>21</sup> D. Schläpfer, 1998: Differential Absorption Methodology for Imaging Spectroscopy of Atmospheric Water Vapor. *Remote Sensing Series*, RSL, Zurich, Vol. 32, pp. 131.
- <sup>22</sup> D.J. Diner, C.J. Brügge, J.V. Martonchik, T.P. Ackerman, R. Davies, S.A.W. Gerstl, H.R. Gordon, P.J. Sellers, J. Clark, J.A. Daniels, E.D. Danielson, V.G. Duval, K.P. Klaasen, G.W. Lilienthal, D.I. Nakamoto, R.J. Pagano, and T.H. Reilly, “MISR: A Multiangle Imaging SpectroRadiometer for Geophysical and Climatological Research from EOS,” *IEEE T. Geosc. Remote Sens.*, IEEE, **27(2)**, 200-214 (1989).
- <sup>23</sup> ESA: *SPECTRA-Surface Processes and Ecosystem Changes Through Response Analysis* (Reports for Assessment: The five Earth Explorer Core Missions, ESA SP-1257(5), 2001)

## TABLES

**Table 1: Applications and variables used for the model.**

<b>Application</b>	<b>No. of Vars</b>	<b>Variables listing</b>	<b>Model/Reference</b>	<b>Sun Zenith</b>	<b>Ground Altitude</b>
Vegetation	3	Leaf chlorophyll, leaf water, leaf area index	PROSPECT/SAIL <sup>15, 16</sup> reflectance <sup>17</sup>	0, 18, 48	0.2 km
Limnology	2	Chlorophyll A, Particulate Matter	Keller <sup>18</sup> remote sensing water surface reflectance	0, 27, 70	0.2 km
Snow	2	Snow grain size, snow optical thickness	Painter <sup>19</sup> reflectance	29	2.9 km
Geology	6	Chlorite, Epidote, Montmorillonite, Kaolinite, Calcite, Jarosite	Linear mixing <sup>20</sup> reflectance	0, 18, 48	0.2 km
Atmosphere	3	Aerosol optical thickness, Aerosol model, Water vapor	MODTRAN4 <sup>10</sup> radiance <sup>21</sup>	0, 18, 48	0.2 km
Calibration	2	SNR at minimum and at maximum radiance level of characterized sensors	Various Sensors <sup>14</sup>	n.a.	n.a.

## LIST OF FIGURES

1. Workflow for the derivation of critical radiometric signatures, noise equivalent radiance, and SNR values.
2. Relation between  $L$  and  $\Delta L$  at 560 nm wavelength for 'Leaf Chlorophyll'. A fit of a square root function is used to derive the lower limitation of the cloud (lower curve).
3. Reflectance signatures and modeled at-sensor radiance signature for vegetation parameters. The levels of reflectance and radiance are shown in the left figures, while the respective delta-signatures for the variable 'Leaf Chlorophyll' are given in the two plots to the right.
4. Normalization of the vegetation variables 'Leaf Chlorophyll', 'LAI' (Leaf Area Index), and 'Leaf Water' to median radiance levels at two exemplary wavelengths. The square-root normalization function is fitted to the lower boundary of the signature points in the  $L/\Delta L$ -space. Fitting points are indicated by squares on the curves.
5. Selection of relevant signatures for vegetation variables 'Leaf Chlorophyll', 'Leaf Water' and 'Leaf Area Index'. Top: normalized signatures at median radiance conditions, Middle: relative signature strength for each variable with potential exclusion levels. Bottom: selected signatures after applying the 20% exclusion level.
6. Generic minimum, median, and maximum radiance levels for all applications including a MODTRAN simulation for a theoretical minimum (0% reflectance) and maximum (100% reflectance) situation.
7. Delta radiance requirements (equivalent to NedL) as derived from combination of all variables at median radiance level in comparison with cross-calibration requirements. The results are given at the 20% exclusion level, smoothed by a 30 nm averaging filter.
8. SNR requirement for all applications at median radiance on three signature exclusion levels (smoothed by a 30 nm filter).
9. SNR requirement for APEX at median radiance conditions, smoothed by a 30 nm filter (Top). Bottom: wavelength dependent driver applications (unsmoothed).

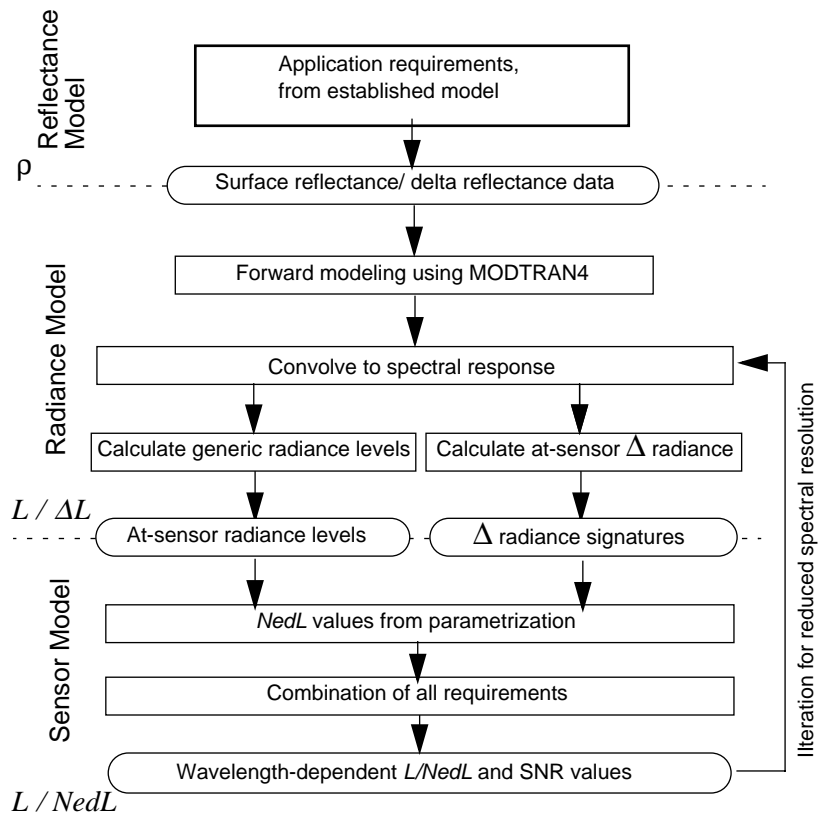
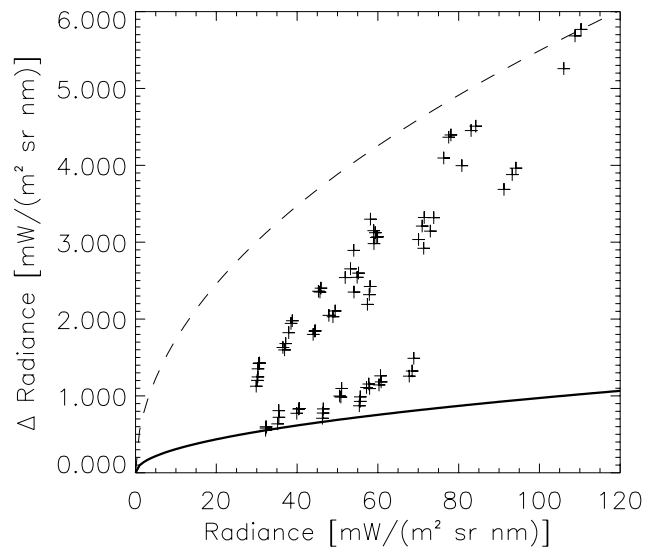


Figure 1: Workflow for the derivation of critical radiometric signatures, noise equivalent radiance, and SNR values.



---

Figure 2: Relation between  $L$  and  $\Delta L$  at 560 nm wavelength for 'Leaf Chlorophyll'. A fit of a square root function is used to derive the lower limitation of the cloud (lower curve).

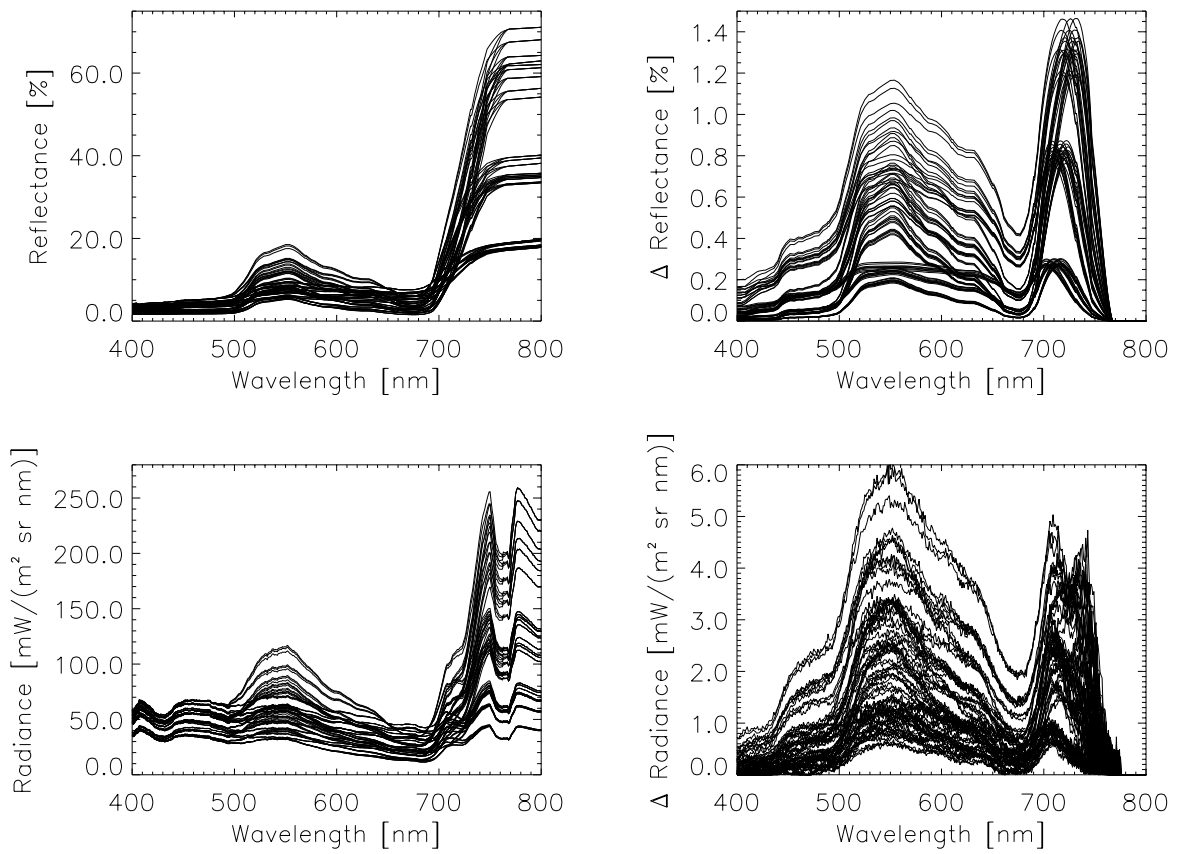


Figure 3: Reflectance signatures and modeled at-sensor radiance signature for vegetation parameters. The levels of reflectance and radiance are shown in the left figures, while the respective delta-signatures for the variable 'Leaf Chlorophyll' are given in the two plots to the right.

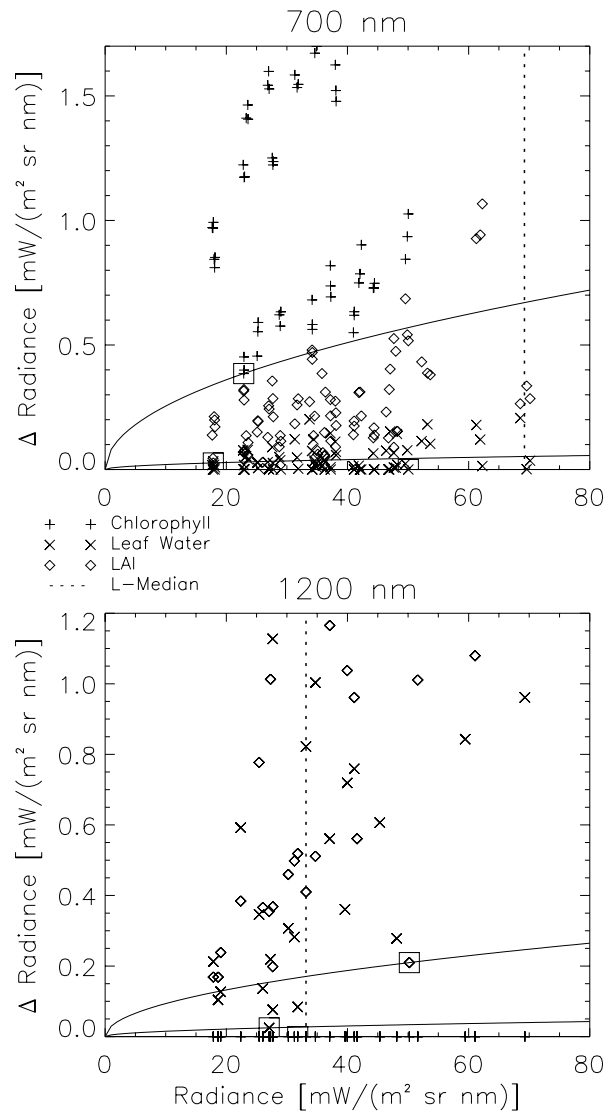


Figure 4: Normalization of the vegetation variables ‘Leaf Chlorophyll’, ‘LAI’ (Leaf Area Index), and ‘Leaf Water’ to median radiance levels at two exemplary wavelengths. The square-root normalization function is fitted to the lower boundary of the signature points in the  $L/\Delta L$ -space. Fitting points are indicated by squares on the curves.

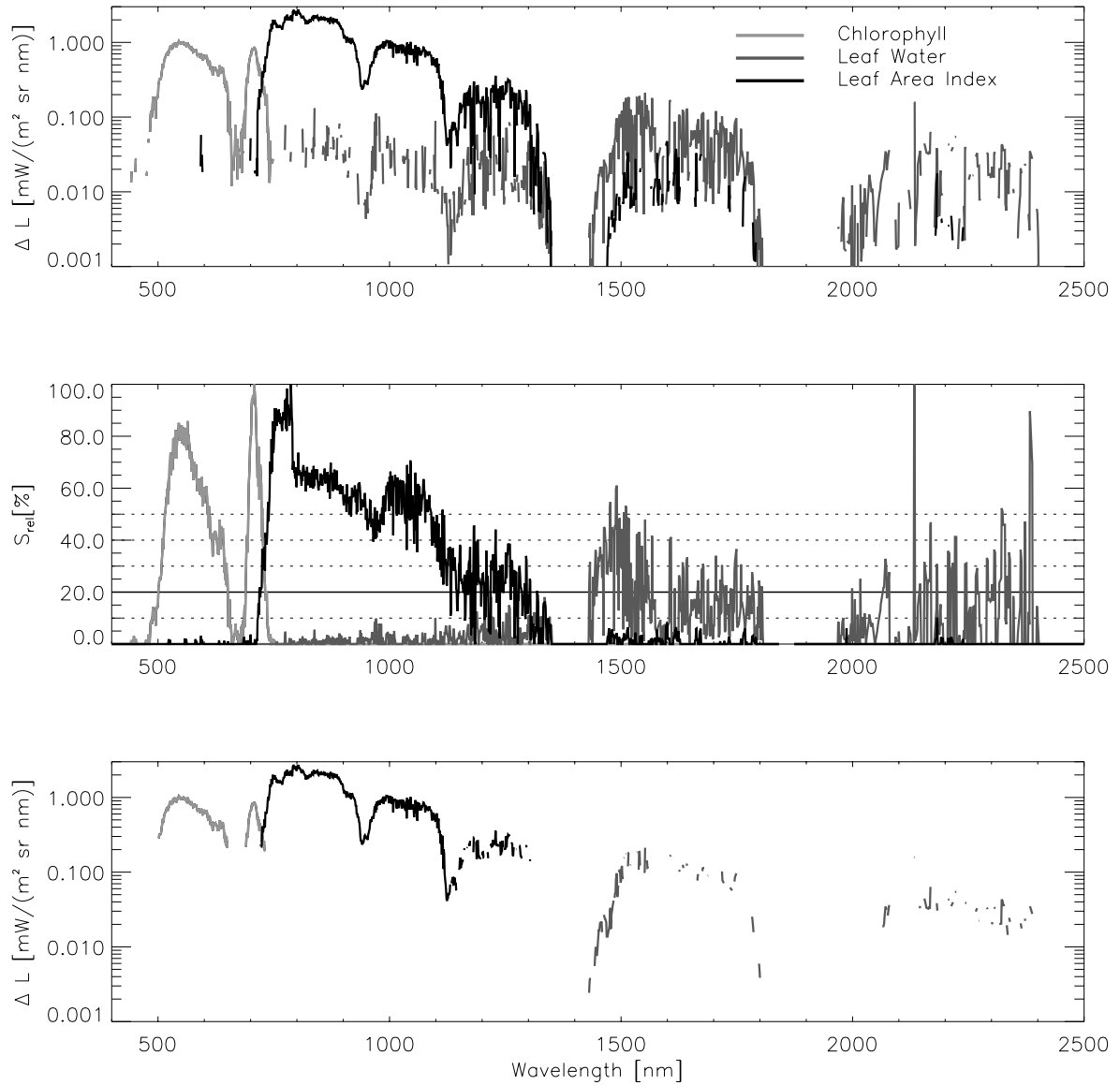


Figure 5: Selection of relevant signatures for vegetation variables ‘Leaf Chlorophyll’, ‘Leaf Water’ and ‘Leaf Area Index’. Top: normalized signatures at median radiance conditions, Middle: relative signature strength for each variable with potential exclusion levels. Bottom: selected signatures after applying the 20% exclusion level.



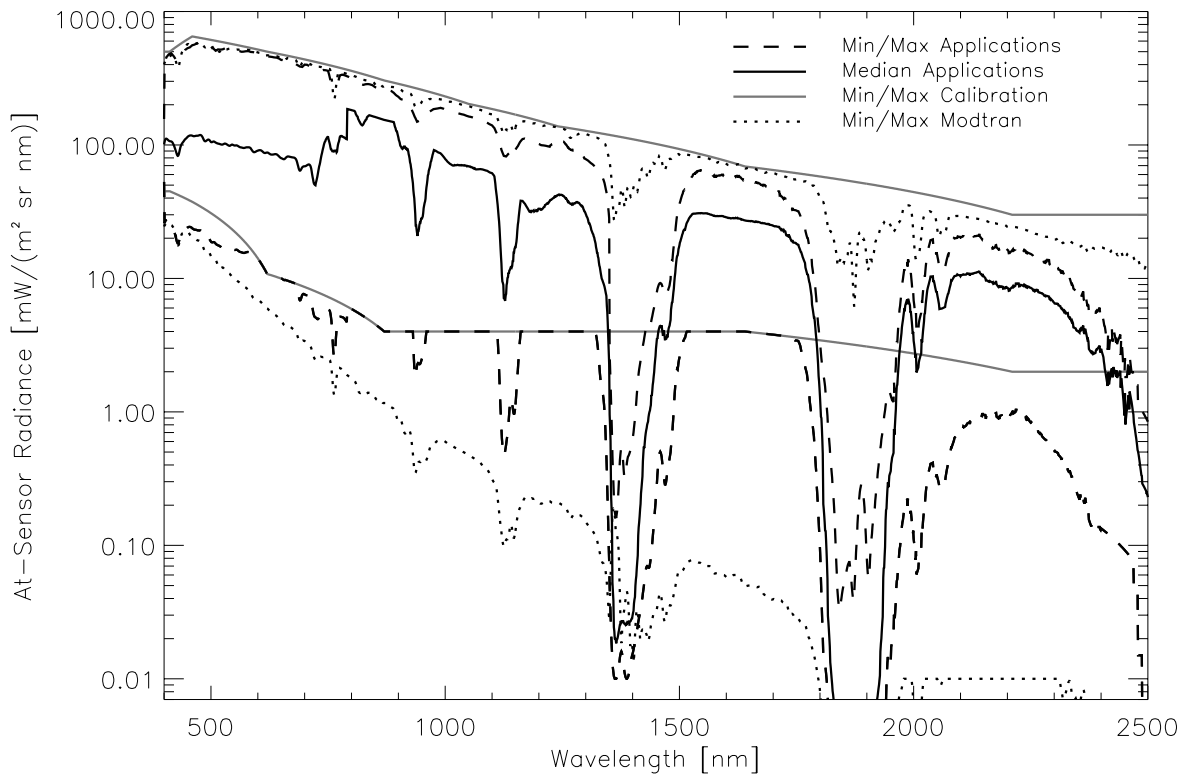
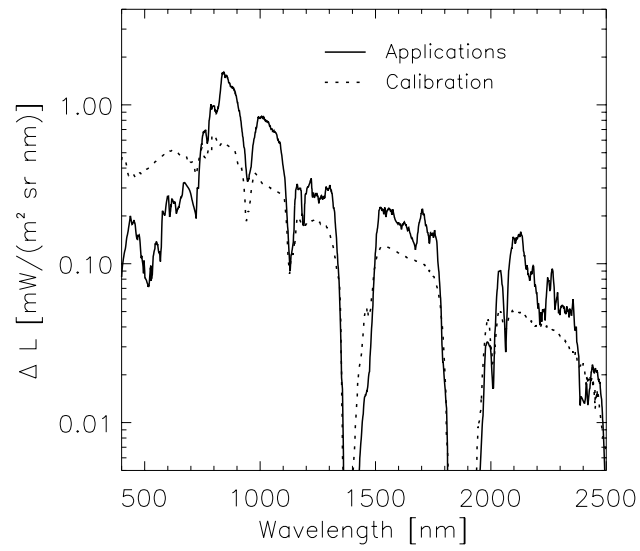
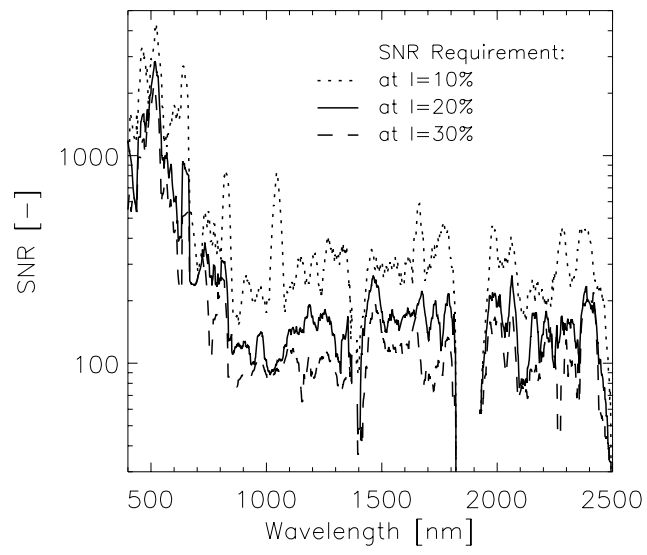


Figure 6: Generic minimum, median, and maximum radiance levels for all applications including a MODTRAN simulation for a theoretical minimum (0% reflectance) and maximum (100% reflectance) situation.



---

Figure 7: Delta radiance requirements (equivalent to NedL) as derived from combination of all variables at median radiance level in comparison with cross-calibration requirements. The results are given at the 20% exclusion level, smoothed by a 30 nm averaging filter.



---

Figure 8: SNR requirement for all applications at median radiance on three signature exclusion levels  $l$  (smoothed by a 30 nm filter).

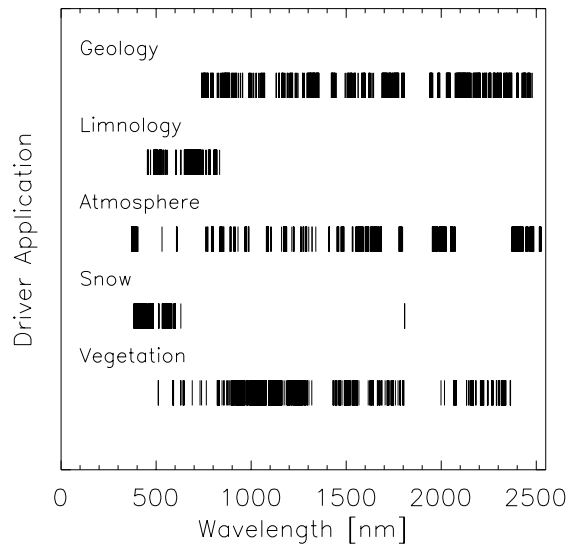
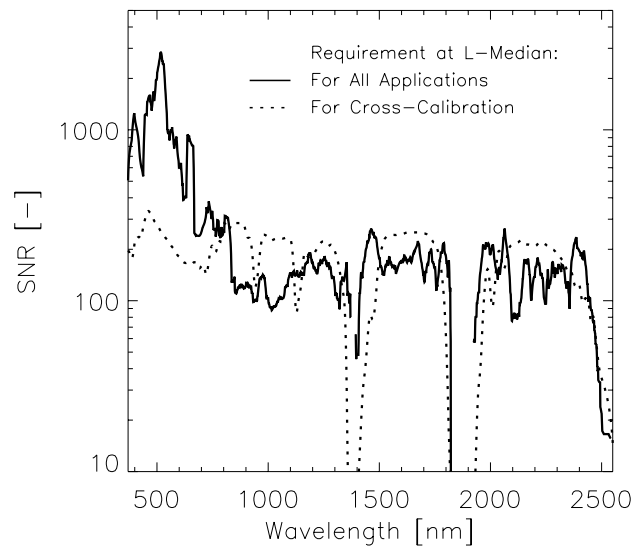


Figure 9: SNR requirement for APEX at median radiance conditions, smoothed by a 30 nm filter

(Top). Bottom: wavelength dependent driver applications (unsmoothed).